ISBN: 978-3-95450-191-5 doi:10.18429/JACoW-SRF2017-FRXAA02

HIGH-EFFICIENCY, HIGH-CURRENT OPTIMIZED MAIN-LINAC ERL CRYOMODULE*

F. Furuta, N. Banerjee, A. Bartnik, J. Dobbins, R. Eichhorn, M. Ge, G. Hoffstaetter, M. Liepe, P. Quigley, D. Sabol, J. Sears, E. Smith, V. Veshcherevich, CLASSE, Cornell University, USA

Abstract

The Main Linac Cryomodule (MLC) prototype is a key component of the Cornell-BNL ERL Test Accelerator (CBETA) project, which is a 4-turn FFAG ERL currently under construction at Cornell University. This novel cryomodule is the first SRF module ever to be fully optimized simultaneously for high efficient SRF cavity operation and for supporting very high CW beam currents. After a successful initial MLC testing, the MLC has now been moved into its final location for the CBETA ring. For a first beam test of the MLC and CBETA, the Cornell ERL high voltage DC gun and SRF injector cryomodule were connected to MLC via an entry beam line; a beam stop assembly was also installed at the exit line. In this paper, we summarize the performance of this novel ERL cryomodule including results of the first beam test and additional tests focused on RF field stability and cavity microphonics.

INTRODUCTION

The Cornell-BNL ERL Test Accelerator (CBETA) is a collaboration project between BNL and Cornell to investigate eRHIC's non-scaling Fixed Field Alternating Gradient (NS-FFAG) optics and its multi-turn Energy Recovery Linac (ERL) by building a 4-turn, one-cryomodule ERL at Cornell (Fig. 1) [1-3]. CBETA will be built in the L0E area of Wilson Lab at Cornell with many components that have been developed at Cornell under previous R&D programs for a hard x-ray ERL [4].

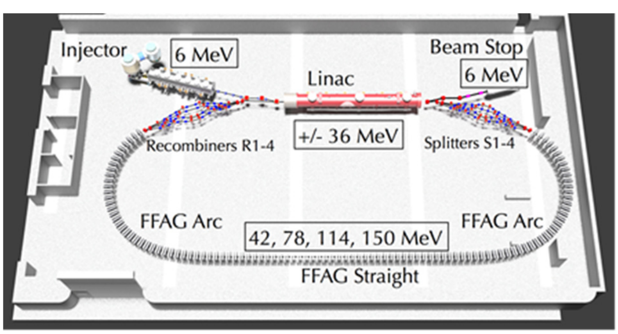

Figure 1: The layout of CBETA project at Cornell.

The main accelerator module, one of the key components for CBETA, will be the Cornell Main Linac Cryomodule (MLC) which will provide 36MeV beam energy gain per pass through the MLC. The MLC was built as a prototype for the Cornell hard x-ray ERL project and designed to operate in CW at 1.3GHz with 2ps bunch length, normalized emittance of 0.3mm-mrad, and 100mA average current in each of the accelerating and decelerating beams [5]. Some other key components, such as the Cornell high voltage DC-gun, Injector Cryomodule (ICM), and Beam stop, shown in Fig. 1, already exist at Cornell, have been commissioned, and are ready for CBETA. In this paper, we report on initial commissioning test results of the MLC, microphonics studies and its compensations, and initial beam acceleration test through the MLC.

MAIN LINAC CRYOMODULE PROTOTYPE

Figure 2 shows an image of the Main Linac Cryomodule prototype in its final location for the CBETA ring. The design of the MLC for the Cornell ERL had been completed in 2012 [4]. One of the unique design goals of the MLC is a combination of a high cavity quality factor Q_0, targeted 2×10^{10} at 16.2MV/m, 1.8K, and a high loaded-Q design of $\sim6\times10^7$, which is equivalent to a narrow half bandwidth of ~10Hz. In order to meet strict beam energy stability requirements, the required amplitude stability and phase stability are 1×10^{-4} in rms and 0.05° in rms, respectively. In addition, as a high current machine, the suppression of high order modes (HOMs) excited by the beam in the SRF cavities in the MLC is also essential.

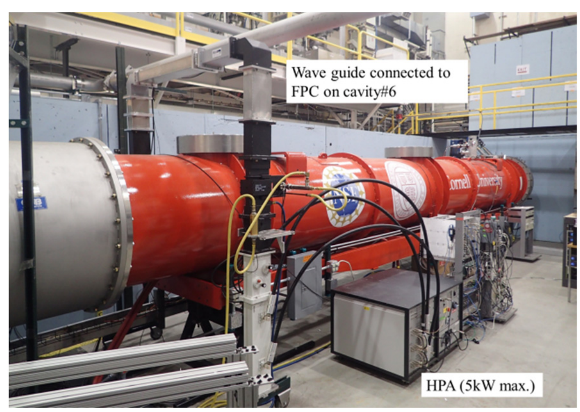

Figure 2: The MLC prototype in its final location.

A general description of the MLC is given in the following. The MLC is 9.8m long and houses six 1.3GHz 7-cell superconducting cavities. Three of them are stiffened cavities, and another three are un-stiffened. Individual HOM beamline absorbers are located between the cavities. Each cavity has a single 10kW coaxial RF input coupler, which transfers power from a solid-state RF power source to the cavity (the designed Q_{ext} of RF input coupler is 6.5×10^7). The fabrication and testing of MLC

* This work was performed with the support of NYSERDA (New York State Energy Research and Development Agency) and of the National Science Foundation (Award No. NSF-DMR 0807731).
#ff97@cornell.edu

ISBN: 978-3-95450-191-5 doi:10.18429/JACoW-SRF2017-FRXAA02

components (cavity, high power input coupler, HOM dampers, tuners, etc.), and assembly of the MLC cold mass had been completed from 2013 to 2014 [6-8]. The key parameters of the MLC and the MLC cavity surface preparation are summarized in Table 1 and Table 2, respectively. The MLC was moved into the South-West area of L0E first in early 2015 for initial commissioning test. After the success of initial commissioning test [9-11], the MCL was moved into its final location in early 2017.

Table 1: The MLC Prototype Parameters

Item	Parameter
Number of 7 cell cavities	6
Accelerating gradient	16.2MV/m
R/Q (linac definition)	774 Ohm
Q_{ext}	6.5×10^7
Total 2K/5K/8K loads	76 W / 70 W / 150 W
Number of HOM loads	7
HOM power per cavity	200 W
Couplers per cavity	1
RF power per cavity	10 kW max.
Amplitude/phase stability	10^{-4} / 0.05° rms
Module length	9.8 m

Table 2: Surface Preparation of the MLC Cavities

Process	Parameter
Bulk BCP	140 µm
Degassing	650 degC, 4days
Frequency tuning	Field flatness >90%
Light BCP	10 µm
Baking	120degC, 48hrs
HF rinse	10 min.

INITIAL COMMISSIONING OF THE MLC

Initial commission of the MCL including initial cooldown, RF tests, thermal cycles, slow tuner test, HOM scan and analysis, and LLRF test have been performed during 2015 to 2016. Some details of these tests are described in this section. LLRF testing is discussed in a later section.

RF Tests of the MLC Cavities

Currently only one 5kW High Power Amplifier (HPA) is available for the MLC RF test, so we performed one-by-one RF tests of all six cavities at 1.8K after different cool down conditions. The 7-cell cavities in the MLC on average have achieved successfully the specification values of 16.2MV/m with Q_0 of 2.0×10^{10} at 1.8K. Figure 3 summarizes the maximum field gradient performance and intrinsic quality factor Q_0 (1.8K) of the MLC cavities after the thermal cycles and RF processing. The MLC can provide 76MeV energy gain per ERL turn, which significantly exceeds the CBETA requirement of 36MeV per ERL turn.

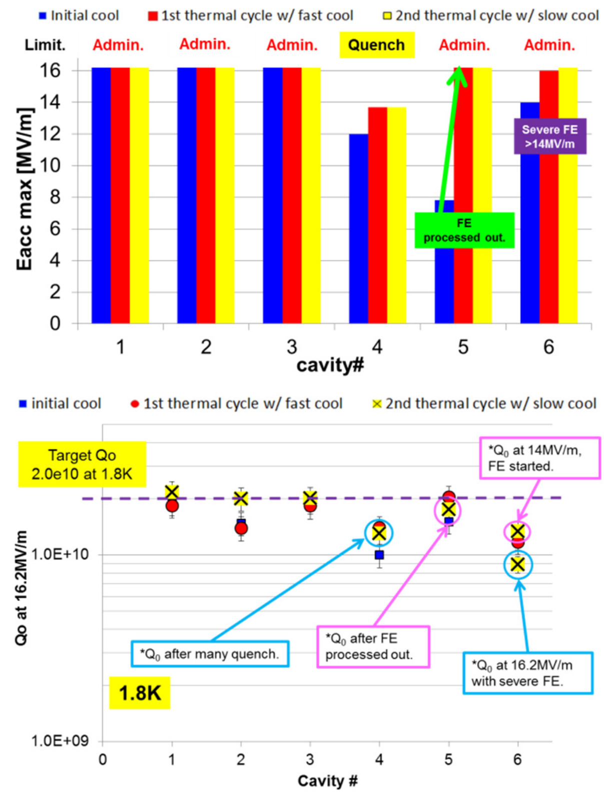

Figure 3: Summary of the performance of the MLC cavities at 1.8K. Top: Maximum fields (primarily administratively limited to 16.2 MV/m). Bottom: Intrinsic quality factors at 1.8K.

The thermal cycles on the MLC cavities show that a slow cool down with a small spatial temperature gradient (ΔT) gave the highest Q_0 for the 7-cell cavities in the MLC prototype. The benefit of slow cool down with smaller ΔT on the MLC is likely due to a suppression of thermal-currents and their induced magnetic fields, which resulted in high Q_0 of cavities in a horizontal cryomodule. It should be noted that a different surface preparation (e.g. nitrogen doping) than what was used for the MLC cavities can instead show optimal performance after fast cool down.

MLC HOM Scans and Analysis

Figure 4 shows a comparison of the measured and simulated MLC HOM loaded quality factors (Q_L). The purple squares show the Q_L results from the HOM scans of cavity #5. The blue data points show Q_L values of dipole modes from the simulations for an MLC cavity with HOM dampers. The comparison indicates (1) scanned HOM frequencies agreed well with simulation results, (2) Q_L of dipole HOMs of the MLC cavities are strongly damped below the target value of ~10^4, and (3) the higher Q modes measured in the MLC are very likely from quadrupole and sextuple modes, as their frequencies line up very well with the simulated frequency bands for these modes, and high Q is expected for these. These mode types are not a concern for causing BBU. The results shown in Fig. 4 also agree well with those from a previ-

ISBN: 978-3-95450-191-5 doi:10.18429/JACoW-SRF2017-FRXAA02

ous HOM study on a prototype 7-cell cavity, which was an un-stiffened cavity in the Horizontal Test Cryomodule (HTC) [12].

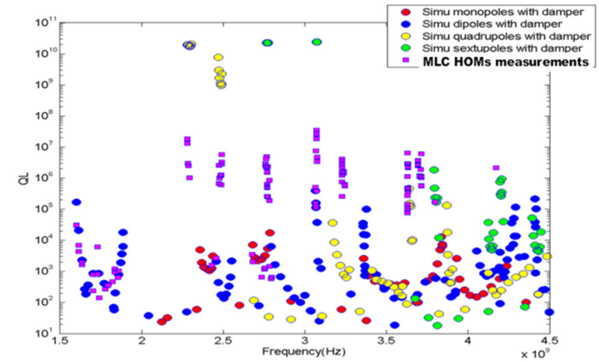

Figure 4: Comparison of MLC HOM measurement results and HOM damping simulation results.

MLC Moving

After the completion of initial commissioning, the MLC was warmed up to room temperature and moved into its final location for the CBETA ring in February 2017 (Fig. 2).

MICROPHONICS IN THE MLC AND ITS COMPENSATION

Microphonics (mechanical cavity vibration) is one of the major sources of frequency perturbation (detuning) and field perturbation of SRF cavities. Another source of detuning is Lorentz Force Detuning (LFD), which is only relevant during times when the cavity accelerating field (V_{acc}) is changing. In this paper, we discuss microphonics in the MLC in its final location and mostly discuss the peak detuning , and not rms values, as the peak detuning determines maximum RF power requirements.

Lorentz Force Detuning and Compensation

Figure 5 shows the measurement results of LFD vs. cavity accelerating field in the MLC cavity #2 (stiffened cavity) and its compensations result. When V_{acc} was ramped up to 4MV, the LFD in the MLC cavity #2 increased to ~30Hz, if no compensation was applied (data set with a red fitting line in Fig. 5). Due to RF power limitation, the Low-Level RF system (LLRF) of the MLC could not sustain the field in the MLC cavity #2 above 4MV without any LFD compensation. To compensate the LFD, a piezoelectric fast tuner was used. A piezo on the MLC cavity #2 was driven by given signal based on Eq. (1), since the LFD is proportional to a square of V_{acc},

$$V_{pz}(t) = aV_{acc}^2 + b \qquad (1)$$

where *a* and *b* is constant. This feedforward compensation worked well. MCL cavity #2 successfully reached 6MV by compensating the LFD with piezo fast tuner (Fig. 5 data set with flat fitting line).

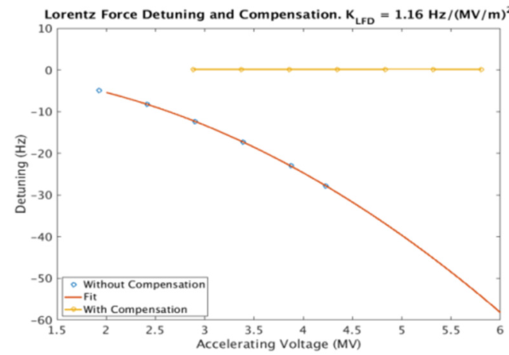

Figure 5; The LFD and its compensation in the MLC cavity #2.

Microphonics Detuning on MLC

Figure 6 shows histograms of the sampled detuning events of each cavity. It has to be pointed out that these microphonics measurements were done in a "mechanically noisy" environment without any optimizations against possible microphonics sources or without applying piezo fast tuner compensation. So far, in final location of the MLC, data sets of two stiffened cavities (cavity #2, #6) and two un-stiffened cavities (cavity #3, #5) were taken [13, 14]. Figure 7 shows integrated detuning vs. vibration frequency of four MLC cavities, which gives a good visualization of the influence of each mechanical vibration excitation [15]. Measured peak detuning and dominant vibration frequencies in each cavity are summarized in Table 3.

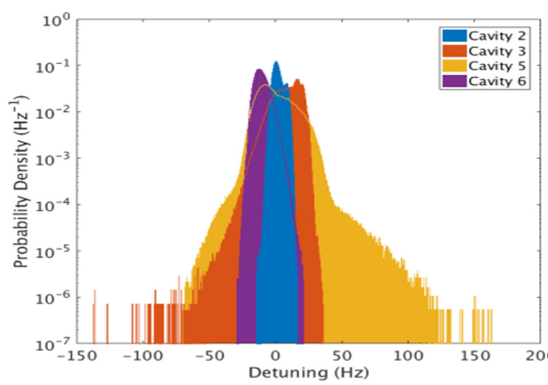

Figure 6: Histogram of the sampled detuning events of MLC cavities [14].

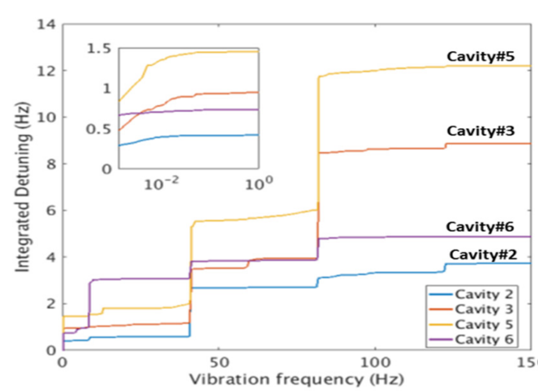

Figure 7: Integrated detuning amplitude [14].

ISBN: 978-3-95450-191-5 doi:10.18429/JACoW-SRF2017-FRXAA02

Table 3: Peak Detuning in the MLC Cavities without Compensation

Cavity#		Peak detuning	Dominant vibration frequency
#2	stiffened	18Hz	40Hz
#3	un-stiffened	137Hz	40, 80Hz
#5	un-stiffened	167Hz	40, 80Hz
#6	stiffened	30Hz	8, 40, 80Hz

Microphonics Sources

Recent progresses on investigations of microphonics sources suggest three dominant vibration sources of microphonics in the MLC [14]: (1) Vibration frequencies of 40 and 80Hz probably come from thermo-acoustic oscillations occurring in cryogenic needle valves on the MLC (Fig. 8, top). (2) Vibration frequency of 8Hz is generated from the pump skid connected to the MLC (Fig. 8, bottom). (3) The peak detuning events are caused by small bubbles generated during the actuation of the pre-cool valve on the MLC (indicated with an arrow in Fig. 8, top). Optimizations of these cryogenic components are in progress.

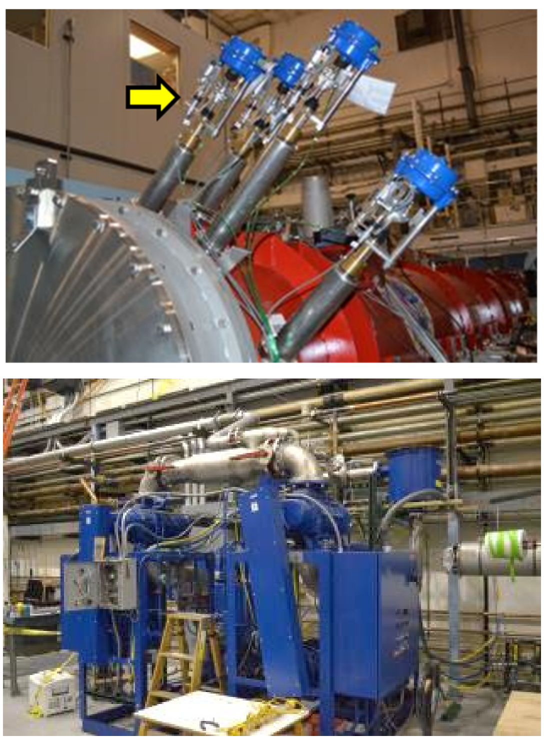

Figure 8: Cryogenic valves on the MCL (top), and pump skid connected to the MLC (bottom).

Compensations of Microphonics in the MLC

In parallel with optimization for the cryogenic scheme and the LLRF system of the MLC, active microphonics compensation using the piezoelectric fast tuner on each MLC cavity has been investigated [13]. Piezo driving signals generated by a proportional integral feedback loop and a feedforward algorithm are applied to the piezo tuner to actively compensate microphonics in the MLC [14]. These algorithms successfully work and reduce the microphonics in the MLC cavity #3 and #6 about a half. The peak detuning of cavity #3 was reduced from 137Hz to 61Hz, and that of the MLC cavity #6 was reduced from 30Hz to 16Hz, so far. Compensation results of MLC cavity #3 and #6 are shown in Fig. 9. For comparison, data sets with and without active compensations are plotted as a histogram of measured detuning events and as an integrated detuning, respectively. We will perform microphonics studies and compensations on the MLC cavity #1 and #4 in the future, and also will revisit the MLC cavity #5, which currently has the worst peak detuning. Further optimizations of the active compensation feedforward and feedback loops are in progress.

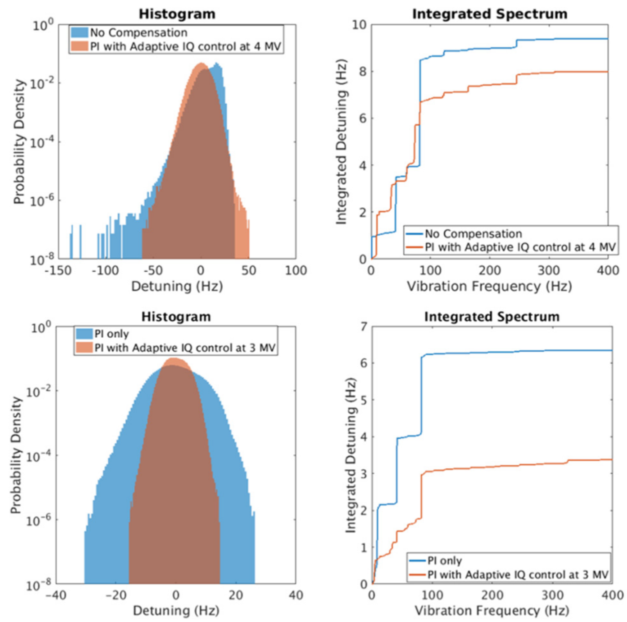

Figure 9: Microphonics compensation results of MLC cavity #3 (top) and MLC cavity #6 (bottom).

RF POWER REQUIREMENT

Figure 10 shows calculations of peak detuning vs. cavity accelerating voltage for various maximum RF input power levels. As an example, these show that the peak detuning needs to be below 54Hz to reach 6MV per cavity with 5kW peak RF power. Current detuning levels of MLC cavity #2 and #6 with microphonics compensation are small enough to reach 6MV, and these cavities have a large overhead on achievable cavity voltage to compensate for un-stiffened cavities, if the microphonics levels cannot be compensated sufficiently to reach 6MV in the un-stiffened cavities. In order to make allowance for the higher microphonics levels of the un-stiffened cavities, three 5kW solid state RF amplifiers (SSAs) for stiffened cavities and three 10kW SSAs for the un-stiffened cavities have been ordered. In addition, a 3 stub waveguide tuner will be installed to each RF input power coupler on MLC cavities, which can be used to reduce the loaded-Q from the design ~6×10^7 to ~2×10^7, and thereby increase the maximum possible energy gain by reducing the required peak power.

ISBN: 978-3-95450-191-5 doi:10.18429/JACoW-SRF2017-FRXAA02

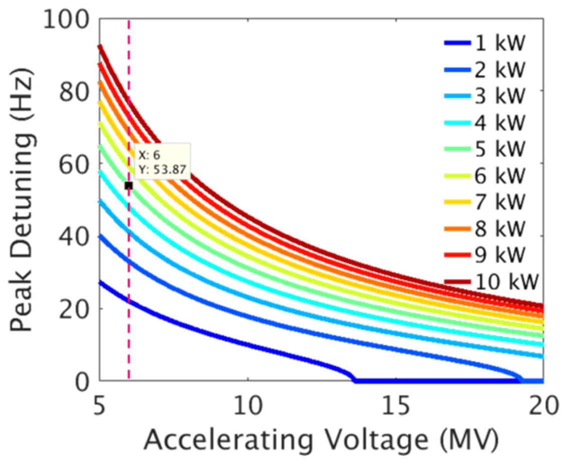

Figure 10: Calculations of allowed peak detuning vs. aimed for cavity accelerating voltage for various peak RF input power levels.

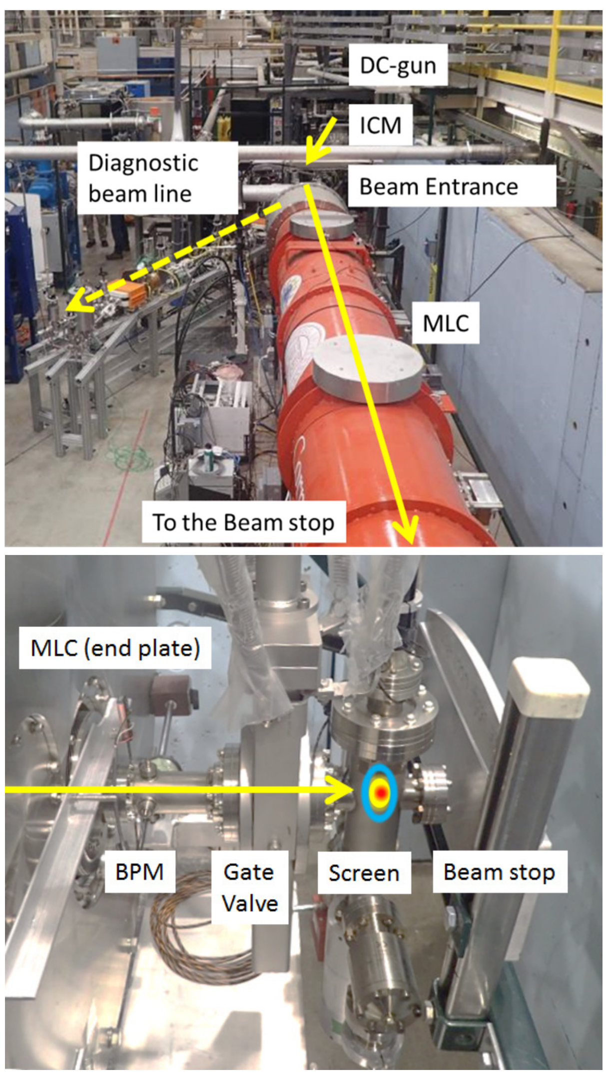

Figure 11: Initial beam acceleration test layout (top), and beam stop assembly (bottom).

INITIAL BEAM ACCELERATION TEST THROUGH MLC

After moving the MCL in its final location, the Cornell ERL high voltage DC gun and Injector Cryomodule (ICM, operation temperature is 2K) were connected to the MLC via the entry beam line (Fig. 11, top), and the beam stop assembly was also installed as the exit line (Fig. 11, bottom).

The MLC was cooled down to 1.8K again prior to initial beam test. Initial beam test has launched in May 2017. The first beam with an energy of 6MeV was passed through the MLC on May 4th, 2017, without active acceleration in the MLC at that moment. After stabilization of the RF field of cavity #2 via the LLRF system with active detuning compensation using the piezoelectric fast tuner, a beam with an energy gain of 12MeV (6MeV from the ICM plus 6MeV from the MLC cavity #2) was transported through the MCL on May 15, 2017. Figure 12 shows the preliminary result of the 12MeV beam image on a beam monitor screen at the beam stop. Another successful 12MeV beam acceleration with the ICM (6MeV) and the MLC cavity #6 (6MeV) was also demonstrated on June 2017.

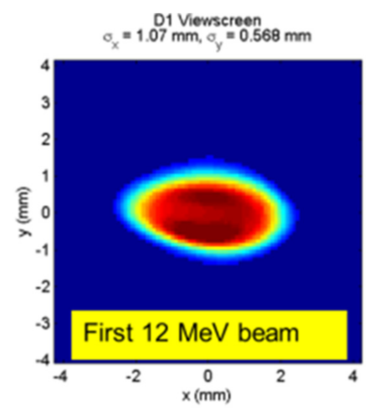

Figure 12: Image of the first 12MeV beam through the MLC on a beam screen.

SUMMARY

The MLC, which is the first high current and high Q_0 linac module ever, has been commissioned successfully. The 7-cell cavities in the MLC can provide an energy gain of up to 76MeV per ERL turn. A new microphonics compensation algorithm has been implemented and is stable and more effective than a traditional feedforward algorithm. A beam with a total energy gain of 12MeV was transported through the MLC, while using active detuning compensation by the piezoelectric tuner, reaching the defined milestone for the initial CBETA beam test. The next milestone for the MLC is to confirm that it can reach the 1st pass total energy gain of 36MeV.

REFERENCES

[1] I. Bazarov *et al.*, "The Cornell-BNL FFAG-ERL Test Accelerator: White Paper", 2014, arXiv:1504.00588.

ISBN: 978-3-95450-191-5 doi:10.18429/JACoW-SRF2017-FRXAA02

[2] G.H. Hoffstaetter *et al.*, "CBETA: the Cornell/BNL 4-turn ERL with FFAG return arcs for eRHIC prototyping", in *Proc. LINAC'16*, East Lansing, MI, USA, Sep. 2016, pp 385-387.

[3] E.C. Aschenauer *et al.*, "eRHIC Design study: an electron-ion collider at BNL", 2014, arXiv:1409.1633.

[4] G.H. Hoffstaetter, S. Gruner, and M. Tigner, eds., "Cornell energy recovery linac project definition design report", `http://erl.chess.cornell.edu/PDDR`

[5] C.E. Mayes *et al.*, "Cornell ERL research and development", in *Proc. PAC'11*, New York, NY, USA, Mar.-Apr. 2011, pp. 729-731.

[6] R. Eichhorn *et al.*, "Design and construction of the main linac cryomodule for the energy recovery linac project at Cornell", in *Proc. SRF'13*, Paris, France, Sep. 2013, pp. 308-313.

[7] R. Eichhorn *et al.*, "Cornell's Main Linac Cryomodule for the Energy Recovery Linac Project", in *Proc. IPAC'14*, Dresden, Germany.

[8] N.R.A. Valles *et al.*, "Record quality factor performance of the prototype Cornell ERL main linac cavity in the horizontal test cryomodule", in *Proc. SRF'13,* Paris, France, Sep. 2013, pp. 300-304.

[9] R. Eichhorn *et al.*, "Cool-down performance of the Cornell ERL cryomodules", in *Proc. LINAC'16*, East Lansing, MI, Sep. USA, 2016, pp 803-805.

[10] F. Furuta *et al*., "Performance of the novel Cornell ERL main linac prototype cryomodule", in *Proc. LINAC'16*, East Lansing, MI, USA, Sep. 2016, pp. 493-496.

[11] M. Ge *et al.*, "Measurements and analysis of cavity microphonics and frequency control in the Cornell ERL main linac prototype cryomodule", in *LINAC'16*, East Lansing, MI, USA, 2016, pp. 489-492.

[12] N. Valles, *et al.*, "HOM studies of the Cornell ERL Main Linac cavity: HTC-1 through HTC-3", in Proc. IPAC2013, Shanghai, China, 2013, pp. 2462-2464.

[13] N. Banerjee *et al.*, "Microphonics Studies of the CBETA Linac Cryomodules", MOPVA122, presented at IPAC'17, Copenhagen, Denmark, 2017.

[14] N. Barnerjee, a presentation at an internal project meeting, unpublished.

[15] A. Neumann, *et al.*, "Analysis and active compensation of Microphonics in continuous wave narrow-bandwidth superconducting cavities", *Phys. Rev. ST Accel. Beams*, vol. 13, p. 082001, Dec. 2010.